R-08-24

Thermal condition of open KBS-3H tunnel

Kari Ikonen, VTT Processes

December 2008

Svensk Kärnbränslehantering AB
Swedish Nuclear Fuel
and Waste Management Co

Box 250, SE-101 24 Stockholm
Phone +46 8 459 84 00

ISSN 1402-3091
SKB Rapport R-08-24

Thermal condition of open KBS-3H tunnel

Kari Ikonen, VTT Processes

December 2008

Keywords: Spent nuclear fuel, Repository, Temperature.

This report is a result of a joint project between Posiva and SKB. This report is also printed as a Posiva report, Posiva 2005-04.

A pdf version of this document can be downloaded from www.skb.se.

Abstract

This report contains the temperature calculations of open KBS-3H type spent nuclear fuel repository, where the fuel canisters are disposed at horizontal position in horizontal tunnels according to the preliminary SKB (Swedish Nuclear Fuel and Waste Management Co) and Posiva plan. The objective of the study is to simulate the operation phase atmospheric conditions in open horizontal tunnels, where the KBS-3H type canister containers and distance blocks are installed. The analyses concern BWR type canisters.

The analyses were made as heat conduction problem by taking into account radiation over gaps. A perforated steel plate surrounds a canister and bentonite. Heat transfer through a perforated plate and surrounding air gaps is a complicated three-dimensional heat transfer problem. To simplify the analysis, the gaps around a container and a distance block were taken into account by describing them by a homogenous layer having effective thermal properties.

Convection due to natural circulation of humid air in horizontal gaps between the container and rock was not considered. Convection could reduce the temperature variation in the gap. On the other hand, the perforated steel plate has good conductivity and transfers quite well heat in horizontal gaps.

Since the actual temperatures of disposal canisters depend in a complicated way on considered time and position, two extreme cases were studied to make the analyses easier. In the first extreme case an infinite queue of canisters are disposed simultaneously. This case overestimates temperatures, since the actual number of canisters is finite and they are not disposed simultaneously. In other extreme case only the first single canister and the first distance block are disposed. This case underestimates temperatures, since the actual number of canisters is greater than one and the canisters heat each other in later phase. The analysis showed that temperatures differ only a little from each other in the two extreme cases. Thus a complicated analysis of several canisters could be avoided. The actual situation is between the two extreme cases and closer to the first case.

According to the analysis the air temperature in the tunnel between the container and rock wall rises to range of 40–50°C within 2–3 weeks after the start of disposal operation. Temperature varies rather much axially in the gap between a container and the rock. In the middle of the canister the average temperature in the gap is about 50°C, whereas in the middle of the distance block the temperature is 24°C. Thus constant humidity conditions are difficult to achieve in the gap between a container and the rock in horizontal direction.

This report is a result of a joint project between SKB and Posiva. This report is also printed as a Posiva report, Posiva 2005-04.

Contents

1 Introduction

The objective of this work is to evaluate the thermal behavior of KBS-3H type spent nuclear fuel repository, where the canisters are disposed at horizontal position in horizontal tunnels. In the base design the Olkiluoto repository is at the depth of 400 m. The analyses concern BWR type canisters. Disposing rate in Posivas's scheme is one canister per week. It takes 25 weeks to dispose all the canisters to one tunnel having 25 canisters.

Figure 1-1 shows the principal dimensions of the horizontal disposal. The canister spacing 11 m is based on earlier analysis /Ikonen 2003b/ to restrict the canister surface to maximum temperature of 90°C, when the canister decay heat is 1,700 W at disposal.

The diameter of the tunnel is 1,850 mm. The length of the BWR canister is 4,800 mm and the diameter 1,050 mm. A canister is disposed in a container, which is covered by perforated steel plate. The length of the container is 5,550 mm. The length of the distance block between containers is 5,450 mm.

The analyses are performed by using axisymmetric heat conduction and radiation models. Canisters do not locate fully coaxially in tunnels due to supporting system. However, for making axisymmetric modeling possible, full axisymmetry is assumed.

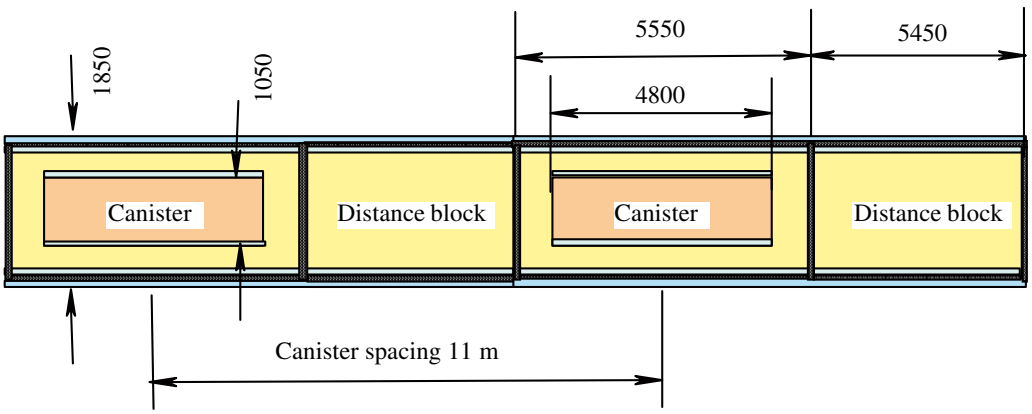

Figure 1-1. *Principal dimensions of horizontal disposal hole, canister and container according to POSIVA's plan.*

2 Initial data

In the following the dimensions of the gaps, thermo-mechanical properties of materials and emissivity of air gap surfaces are presented. The ambient rock temperature in the depth of –400 m is assumed to be +11°C. Decay heat of the BWR fuel is assumed to be 1,700 W at the disposal time and the decrease in time is taken into account as presented in /Ikonen 2003a/. The power remains almost constant during rather short time extending to one year from the disposal time.

2.1 Gap dimensions in horizontal disposal

Figure 2-1 shows the gaps around the canister and the container. All the gaps are conservatively assumed to be air filled. A gap of 3 mm thickness is modeled to exist between the canister and the bentonite buffer. Between the bentonite and the perforated container steel plate a gap of 4 mm thickness is assumed to exist and further between the container steel over pack and the rock the gap thickness is assumed to be 42.5 mm. All these gaps are assumed to be annular. Gaps of 1 mm are assumed axially between bentonite and end steel plates.

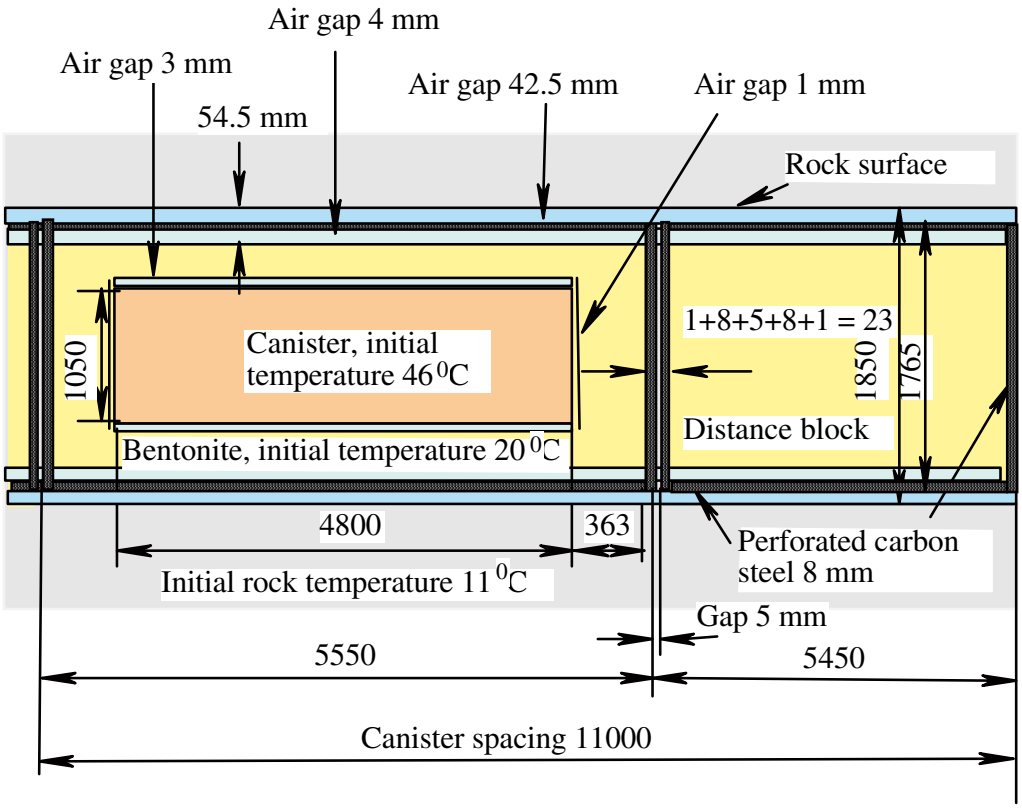

Figure 2-1. *Gap dimensions around canister surface and between buffer and rock.*

2.2 Thermo-mechanical properties of materials

The conductivity of Olkiluoto rock and heat capacity are based on laboratory measurements with core drilled samples /Kukkonen 2000/. The conductivity of the rock decreases slightly as a function of temperature and at temperatures of 22°C, 60°C and 100°C the conductivity is 2.70±0.42, 2.61 and 2.49 W/m/K, respectively. When using low conductivity the temperature of the canister will be conservatively overestimated. **The constant average value of 2.61 W/m/K (at 60°C) is used for all the Olkiluoto repository analysis in this report.**

The heat capacity of the rock increases slightly as a function of temperature and at the temperatures of 22°C, 60°C and 100°C the capacity is 737, 784 and 832±19 J/kg/K, respectively. When using low capacity the temperature of the canister will be conservatively overestimated. **The value of 784 J/kg/K (at 60°C) is used throughout the analysis.** With the rock density of 2,749 kg/m^3 the applied volumetric heat capacity of the rock material is 2.15 MJ/m^3 /K.

The conductivity of the perforated steel plate is assumed to be λ_{steel} = 47 W/m/K /Hökmark and Fälth 2003/.

The conductivity of bentonite buffer depends on saturation rate (Figure 2-2). In normal atmospheric humidity conditions the bentonite conductivity is of about 0.75 W/m/K. In fully dry conditions the conductivity is 0.3 W/m/K and in fully saturated conditions 1.3 W/m/K. In repository condition the effective conductivity of bentonite is estimated to be 1.0 W/m/K. **This value 1.0 W/m/K is used throughout the analysis.**

Figure 2-3 shows the conductivity of air and humid air (relative humidity 100%) as a function of temperature. The curves are nearly same lower temperatures. The lower curve in Figure 2-3 is approximated by the polynomial

$$\lambda(T) = 0.0243 + 9.0381\cdot10^{-5}\,T - 4.7101\cdot10^{-7}\,T^2\ . \qquad (1)$$

This fitting is used in the analyses. All the gaps are assumed to be filled by humid air.

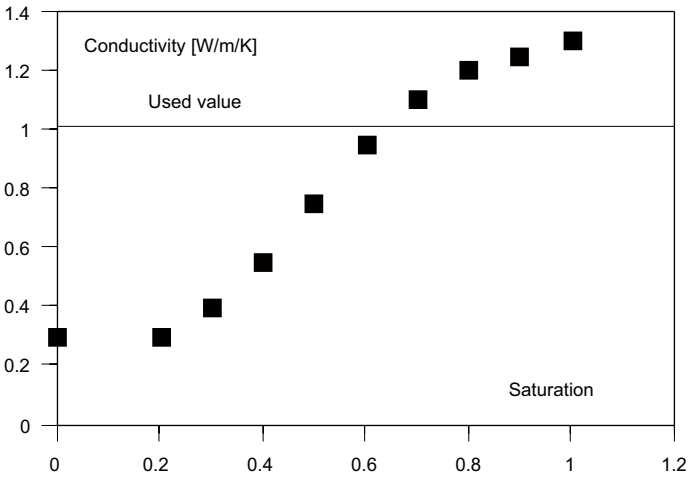

Figure 2-2. *Conductivity of bentonite.*

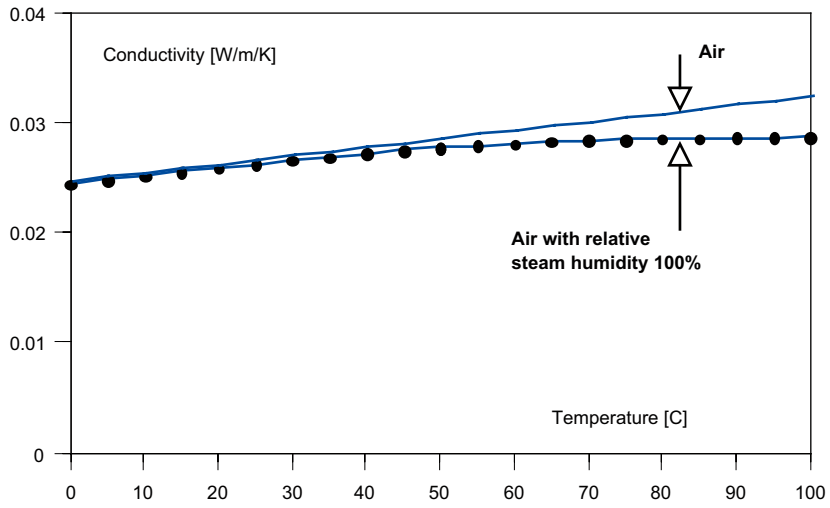

Figure 2-3. *Conductivity of air (continuous line) and humid air (dotted line) in atmospheric pressure.*

2.3 Emissivity of air gap surfaces

The radiation heat flux ϕ_{rad} between two parallel surfaces having temperatures of T_1 and T_2 is calculated from

$$\phi_{rad} = \varepsilon_{tot}\ \sigma(T_1^4 - T_2^4)\ , \tag{2}$$

where the total emissivity is calculated from approximate formula /Ryti 1973/

$$\varepsilon_{tot} = \frac{1}{\frac{1}{\varepsilon_1} + \frac{1}{\varepsilon_2} - 1} = \frac{\varepsilon_1\ \varepsilon_2}{\varepsilon_1 + \varepsilon_2 - \varepsilon_1\ \varepsilon_2}, \tag{3}$$

where ε_1 and ε_2 are the emissivities of the surfaces. The Stefan-Bolzmann constant is $\sigma = 5.6697 \cdot 10^{-8}$ W/(m^{2}K^4).

The emissivity of copper surface depends strongly on the quality of the surface. Polished surface has an emissivity of about 0.02, clean machined surface maybe 0.3, oxidised surface 0.6 /Technical handbook 1973/. If the emissivity of the copper is 0.6 and the emissivity of the bentonite is 0.8, the total emissivity is 0.52. For the total emissivity a value of 0.5 for the gaps around the canister is used throughout the analyses of this report.

For the emissivity of all other surfaces outside of canister copper surface a value 0.8 is applied. This gives for the total emissivity $\varepsilon_{tot} = 1/(1/0.8 + 1/0.8 - 1) = 0.67$. This value is applied between two adjacent surfaces formed of bentonite, perforated steel plate or rock.

3 Calculation methodology

In the actual disposal the canisters do not locate fully coaxially in tunnels due to supporting system. The gaps around the circumference between a container and a tunnel are thus not of uniform width. However, for making axisymmetric modeling possible, the gaps are assumed to be of uniform width around the entire circumference. The analyses are performed by axisymmetric models by control volume method described in /Ikonen 2003a/.

Heat transfer across the air-filled gap will take place by conduction, radiation and convection. The effect of convection is conservatively neglected, since the gaps are rather small and the surfaces are rough and further, the perforated steel plate in horizontal gaps between a container and the rock has good conductivity and transfers quite well heat in horizontal gaps.

3.1 Effective conductivity and capacity of perforated container plate and surrounding gaps

The container is covered by a perforated steel plate of 8 mm. Holes of diameter 100 mm (Figure 3-1) cover 62% both of the cylindrical surface and the end plates. The perforated plate with surrounding humid air gaps is modeled by a single homogeneous layer having effective conductivity and capacity.

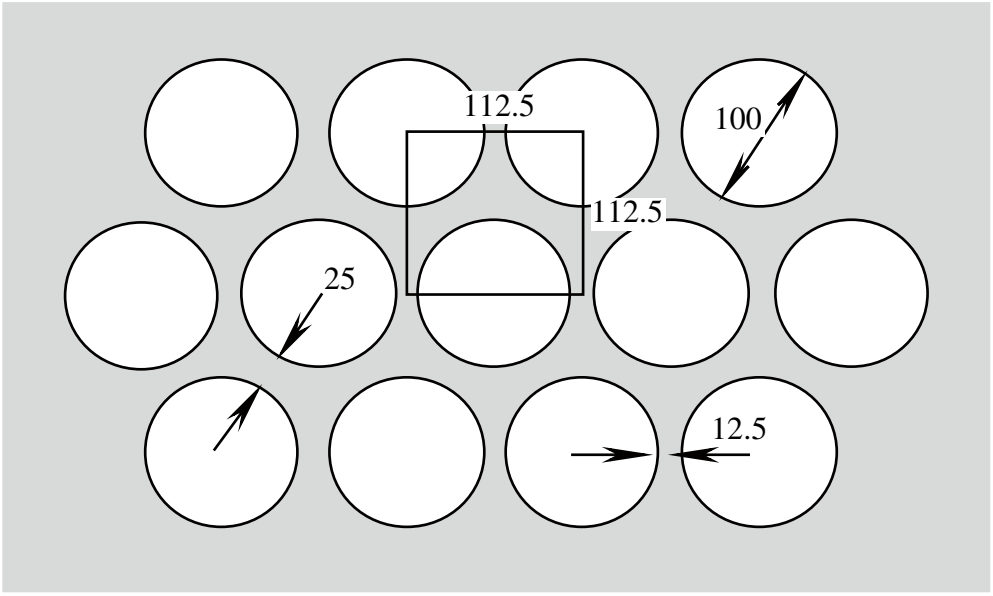

Figure 3-1. *Perforated container plate with holes.*

3.1.1 Transverse effective conductivity

Heat transfer through a perforated plate and surrounding gaps is a complicated situation, whose accurate solution would need three-dimensional analysis. To simplify the analysis, the gaps around a container and a distance block are taken into account by describing them by a homogenous layer having effective thermal properties.

In order to evaluate the contributions of conductive heat transfer in humid air in a gap and of radiative heat transfer between the gap surfaces, the effect of the perforated steel plate in the gap is first omitted. Three gap thicknesses of 4 + 8 + 42.5 mm = 54.5 mm (in the cylindrical part of the container), 1 + 8 + 5 + 8 + 1 mm = 23 mm (in adjacent ends of two containers) and 5 + 8 + 1 mm = 14 mm (related to the end of the first disposed container against the rock, see Chapter 5) are studied. The conduction heat flux ϕ_{air} in humid air and radiation heat flux ϕ_{rad} between two parallel surfaces having temperature differences ΔT are calculated from (omitting interaction between conduction and radiation)

$$\phi_{air} = \lambda(T)\frac{\Delta T}{\delta}$$
$$\phi_{rad} = 4\ \varepsilon_{tot}\ \ \sigma T^3 \Delta T\,. \qquad (4)$$

For the conductivity of humid air the curve in Figure 2-3 is applied and for the total emissivity a value ε_{tot} = 1/(1/0.8 + 1/0.8 – 1) = 0.67 is used. Figure 3-2 shows the ratio of the heat fluxes expressed by Equations (4). In case of wide gap the radiative heat flux is much greater than the conductive heat flux in humid air. Thus it is important to take into account the direct radiation through the holes in perforated steel plates.

In the following the perforated steel plate is taken into account and it is conservatively assumed that the holes and gaps are air-filled. A single layer having effective conductivity and capacity models the area. For determining the effective conductivity of perforated container plate and coaxial annular air gaps it is assumed that through a hole heat is transferred by conduction in air and by radiation between bentonite and rock surfaces (right upwards arrow in Figure 3-3).

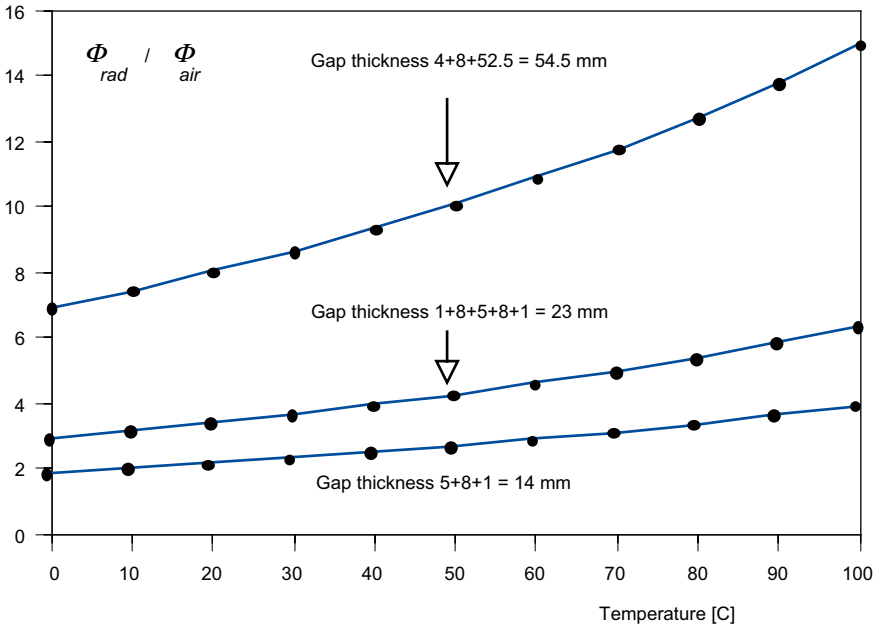

Figure 3-2. *Heat flux ratio for different gap thicknesses.*

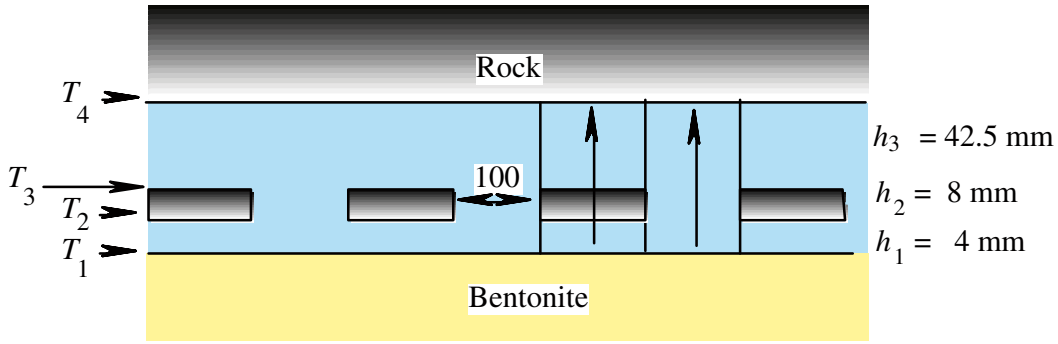

Figure 3-3. *The modeling of effective conductivity of perforated container plate and surrounding air-filled gaps.*

In position of steel (left upwards arrow in Figure 3-3) it is assumed that equal heat flux goes through the internal air gap, through steel thickness and through the external air gap. Heat flow in full air-filled area and steel wall area are summed to determine the effective conductivity. Temperatures T_1, T_2, T_3 and T_4 shown in Figure 3-3 are assumed to be constant in axial (horizontal) direction.

For determining three unknowns T_2, T_3 and λ_{eff} following equations are obtained (neglecting the effect of curvature)

$$\lambda_{air}\frac{T_1 - T_2}{h_1} + \varepsilon_{tot}\ \sigma(T_1^4 - T_2^4) = \lambda_{steel}\frac{T_2 - T_3}{h_2} = \lambda_{air}\frac{T_3 - T_4}{h_3} + \varepsilon_{tot}\ \sigma(T_3^4 - T_4^4)$$
$$\lambda_{eff}\frac{T_1 - T_4}{h_1 + h_2 + h_3} = 0.38\ \lambda_{steel}\frac{T_2 - T_3}{h_2} + 0.62\ [\lambda_{air}\frac{T_1 - T_4}{h_1 + h_2 + h_3} + \varepsilon_{tot}\ \sigma(T_1^4 - T_4^4)]\ . \qquad (5)$$

The thickness values are $h_1 = 4$ mm, $h_2 = 8$ mm and $h_3 = 42.5$ mm. At 50°C the conductivity of air is about 0.03 W/m/K and the conductivity of carbon steel is assumed to be 47 W/m/K. For the emissivity of all surfaces a value 0.8 is applied.

This gives for the total emissivity $\varepsilon_{tot} = 1/(1/0.8 + 1/0.8 - 1) = 0.67$. It should be emphasized that Equations (5) are not exact but approximate.

The upper curve with dots in Figure 3-4 calculated form Equations (5) shows the effective conductivity λ_{eff} as a function of the average temperature $(T_1 + T_4)/2$. The temperature difference $T_1 - T_4$ has a very small effect on the curve.

The effective conductivity of the 54.5 mm layer of the cylindrical container plate and the surrounding gaps is calculated from a fitting applied in the analysis (the upper dotted curve in Figure 3-4, T in Celsius)

$$\lambda_{eff} = 0.173 + 1.64 \cdot 10^{-3}\ T + 5.78 \cdot 10^{-6}\ T^2\ . \qquad (6)$$

If the steel plate in the gap is omitted, the effective conductivity is calculated from Equations (1)

$$\lambda_{eff} = \delta\frac{\phi_{air} + \phi_{rad}}{\Delta T} = \lambda_{air}(T) + 4\ \delta\varepsilon_{tot}\ \sigma T^3\ . \qquad (7)$$

The two uppermost curves in Figure 3-4 demonstrate that the perforated steel plate decreases the heat flux over the gap of 54.5 mm.

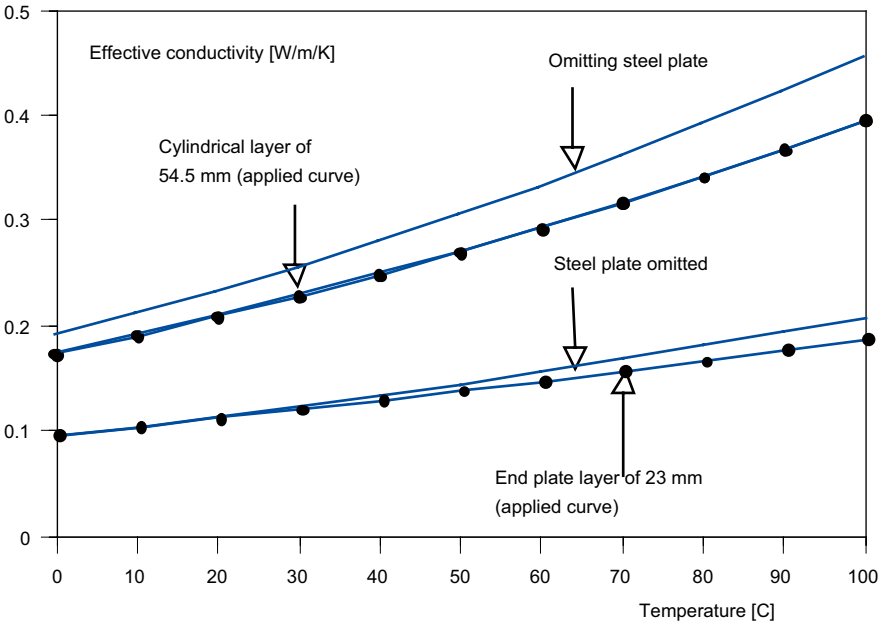

Figure 3-4. *Effective conductivity of perforated container plate and surrounding gaps.*

Similar procedure is applied also in the perforated container end plate having total thickness of 23 mm (Figure 3-5). Between two adjacent container end plates a gap of 5 mm filled with air is assumed. A single layer having effective conductivity and capacity models the area.

If the holes in the end plates are not at same positions, straight air channel is about half of the 62%, i.e. about 31% of the area is covered by air. The area covered by both steel plates is about 38%/2 = 19%. The rest of the area 100%–(31%+19%) = 50% = 25% + 25% is covered by one steel plate.

For determining three unknowns T_2–T_5 and λ_{eff} following equations are obtained requiring heat flux continuity through different layers show by an arrow in Figure 3-5 (neglecting the effect of curvature)

$$\begin{aligned}
&\lambda_{air}\frac{T_1-T_2}{h_1}+\varepsilon_{tot}\,\sigma(T_1^4-T_2^4)=\lambda_{steel}\,\frac{T_2-T_3}{h_2}=\lambda_{air}\frac{T_3-T_4}{h_3}+\varepsilon_{tot}\,\sigma(T_3^4-T_4^4)\\
&=\lambda_{steel}\frac{T_4-T_5}{h_4}=\lambda_{air}\frac{T_5-T_6}{h_5}+\varepsilon_{tot}\,\sigma(T_5^4-T_6^4)\\
&\lambda_{eff}\,\frac{T_1-T_6}{h_1+h_2+h_3+h_4+h_5}=0.19\;\lambda_{steel}\,\frac{T_2-T_3}{h_2}+0.25\;[\lambda_{air}\frac{T_1-T_4}{h_1+h_2+h_3}+\varepsilon_{tot}\,\sigma(T_1^4-T_4^4)]\\
&+0.25\;[\lambda_{air}\frac{T_3-T_6}{h_3+h_4+h_5}+\varepsilon_{tot}\,\sigma(T_3^4-T_6^4)]+0.31\;[\lambda_{air}\frac{T_1-T_6}{h_1+h_2+h_3+h_4+h_5}+\varepsilon_{tot}\,\sigma(T_1^4-T_6^4)]\,.
\end{aligned}\qquad (8)$$

It should be emphasized that these equations are approximate. The lower curve with dots in Figure 3-4 (calculated from Equations (8)) shows the effective transverse conductivity of the end plate layer with total thickness of 23 mm. A fitting applied in the analysis is

$$\lambda_{eff}=0.094+9.14\cdot 10^{-4}\,T\,. \qquad (9)$$

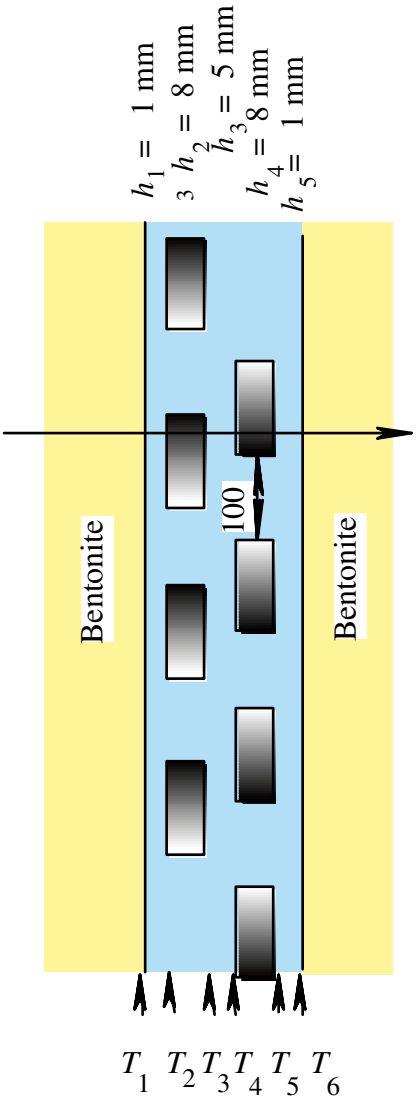

Figure 3-5. *The modelling of effective conductivity of perforated container plate and surrounding air-filled gaps.*

3.1.2 In-plane effective conductivity

Most of the heat is transferred by steel ligaments in the direction of the perforated steel plate (Figure 3-1). Part of the heat is transferred by radiation over holes, but this is significantly less than by conduction in steel, whose conductivity is high (λ_{steel} = 47 W/m/K). The effective in-plane conductivity is calculated as λ_{eff} = (12.5 mm/112.5 mm)·47 W/m/K = 5.2 W/m/K. In the cylindrical gap the air gaps decreases this value further to λ_{eff} = (8 mm/54.5 mm)·5.2 W/m/K = 0.77 W/m/K. In the axial gap the effective conductivity is λ_{eff} = (8 mm + 8 mm)/23 mm·5.2 W/m/K = 3.6 W/m/K. These effective in-plane values are assumed to be isotopic, though actually the conductivity of the perforated plate (Figure 3-1) depends to some extent on the direction.

3.1.3 Effective capacity

The effective volumetric heat capacity is determined by weighting the volumetric capacities of humid air 1,140 J/m^3/K at 40°C and of steel 3.1 MJ/m^3/K. In the cylindrical container plate the volumetric fractions of humid air and steel are (4+0.62·8+42.5)/54.5 = 0.944 and 1 – 0.944 = 0.046 giving for the effective volumetric heat capacity a value of **0.174 MJ/m^3/K**, which is used in the analysis. In the end plate the volumetric fractions are (1+0.62·8+5+0.62·8+1)/23 = 0.735 and 0.264 giving for the effective volumetric heat capacity a value of **0.820 MJ/m^3/K**, which is used in the analysis.

3.1.4 Zero gap

In the end lid of the canister a gap of 1 mm is assumed. For calculational reasons (for avoiding thin grid layers) the gap thickness is assumed to be zero. For the heat flux it may be written

$$\phi = \varepsilon_{tot}\,\sigma(T_1^4 - T_2^4) + \frac{\lambda_{air}}{\delta}(T_1 - T_2)$$
$$= \varepsilon_{tot}\,\sigma\,[1 + \frac{\lambda_{air}}{\varepsilon_{tot}\,\sigma\,\delta(T_1 + T_2)\,(T_1^2 + T_2^2)}]\,(T_1^4 - T_4^4)\,, \tag{10}$$

where T_1 and T_2 are the surface temperatures and δ is the actual gap thickness. For the total emissivity a value of $\varepsilon_{tot} = 0.5$ is used. Figure 3-6 shows the correction coefficient, which becomes rather high.

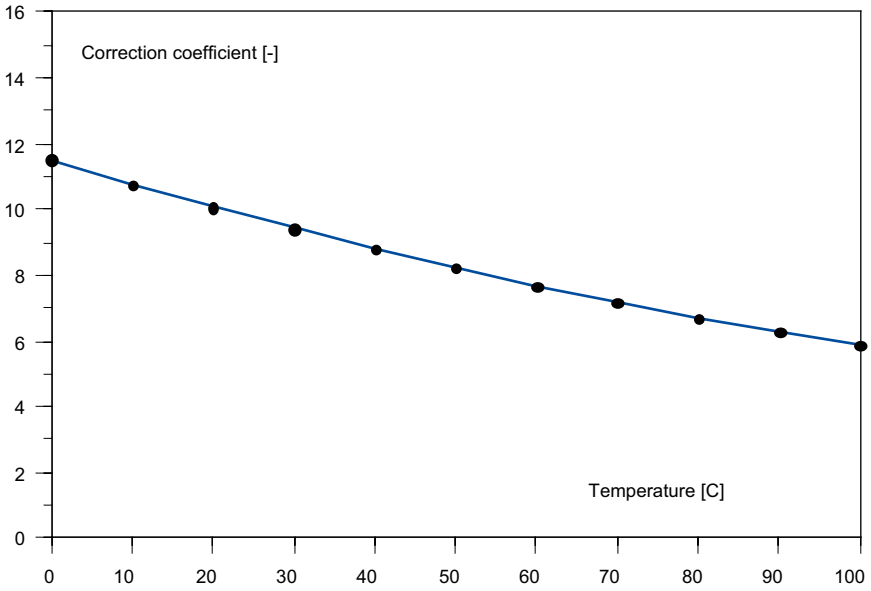

Figure 3-6. *Correction coefficient in Formula (10), when air gap is 1 mm is assumed to have zero thickness in numerical analysis.*

4 Analysis of an infinite queue of canisters

Since the actual temperatures of disposal canisters depend in a complicated way on considered time and position, two extreme cases are studied. In the first extreme case an infinite queue of canisters are disposed simultaneously. This case overestimates temperatures, since the number of canisters is finite and they are not disposed simultaneously. In the other extreme case only the first single canister and the first distance block are disposed. This case underestimates temperatures, since the actual number of canisters is greater than one and the canisters heat each other. It will turn out later in Chapter 5.2 that in these extreme cases temperatures differ only a little from each other. Thus a complicated analysis of several canisters can be avoided. The actual situation is between these extreme cases and closer to the first case.

The canister was assumed to be homogeneous with uniform power generation over its volume and its content was not modeled in detail, since the copper shell has very high thermal conductivity (390 W/m/K) causing nearly uniform temperature distribution on the external surface of the canister.

The volumetric heat capacities of the copper, the cast iron and the Uranium oxide are about 3.4 MJ/m^3/K, 4.1 MJ/m^3/K and 2.8 MJ/m^3/K, respectively. Since there are also voids inside the canister, the average volumetric heat capacity is lower. The average value of 2.4 MJ/m^3/K, taken from /Agelskog and Jansson 1999/, was used in the analyses.

Table 4-1 presents data for the numerical analysis. The radiation is taken into account in the inner canister/buffer air gap in the cylindrical part and on the lids. The outer gap is modeled by a single layer having effective conductivity and capacity as described in Chapter 3.1.

Table 4-1. Initial data for the analysis of infinite queue of canisters with an air gap between the canister and buffer and with a gap between the buffer and the rock in cylindrical part. BWR fuel and Olkiluoto site properties.

Canister spacing	11	m
Decay heat when disposed	1,700	W
Ambient rock temperature	11.0	°C
Canister initial temperature	46.0	°C
Canister length	4.80	m
Canister conductivity	390	W/m/K
Canister volumetric heat capacity	2.4	MJ/m^3/K
Canister radius	0.525	m
Container length	5.55	m
Tunnel radius	0.925	m
Rock conductivity at 60°C	2.61	W/m/K
Rock volumetric heat capacity	2.15	MJ/m^3/K
Bentonite (buffer) conductivity	1.0	W/m/K
Bentonite initial temperature	20.0	°C
Width of air gap on canister surface	3	mm
Width of outer gap area	54.5	mm
Bentonite volumetric capacity	2.2	MJ/m^3/K
Total emissivity over internal air gap	0.5	–

4.1 Modeling dimensions of infinite canister queue

Figure 4-1 shows the infinite canister queue model for numerical analysis.

Figure 4-2 shows the geometry of the modeled area for the numerical analysis. It illustrates also material types. Figure 4-3 shows the initial temperature distribution. In the numerical model the left and right vertical boundaries are assumed to be adiabatic describing an infinite queue of canisters. In the model there are 4,378 control volumes. The time step in fully implicit numerical scheme is 100 s, when time is less than 100 days and 1,000 s, when time is more than 100 days.

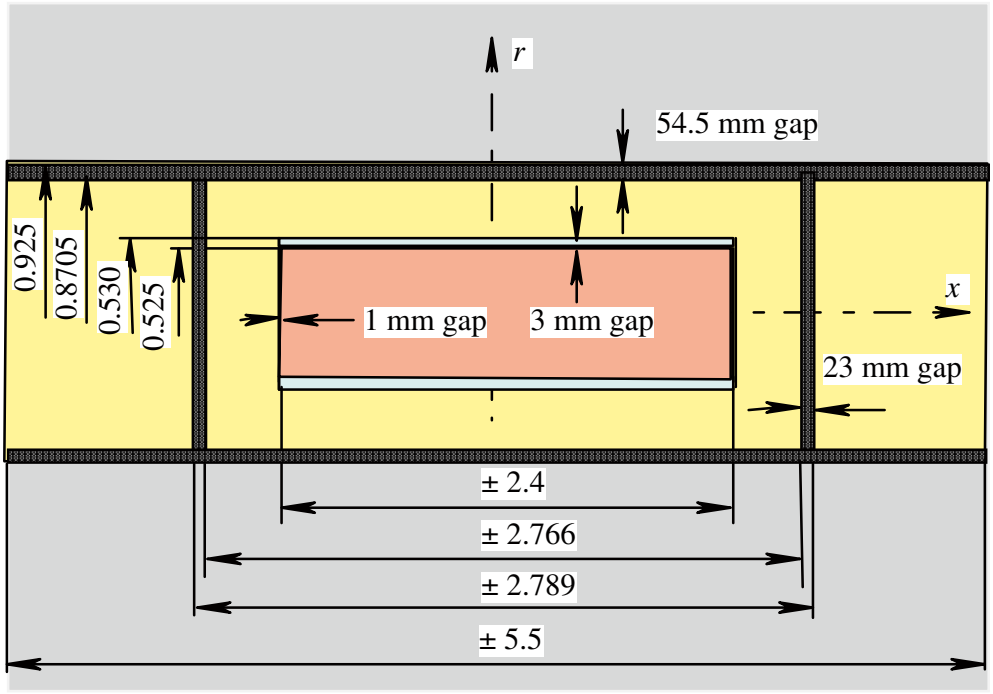

Figure 4-1. *Infinite canister queue model. Dimensions for the model, where right and left vertical planes are thermally insulated/adiabatic corresponding infinite queue of canisters.*

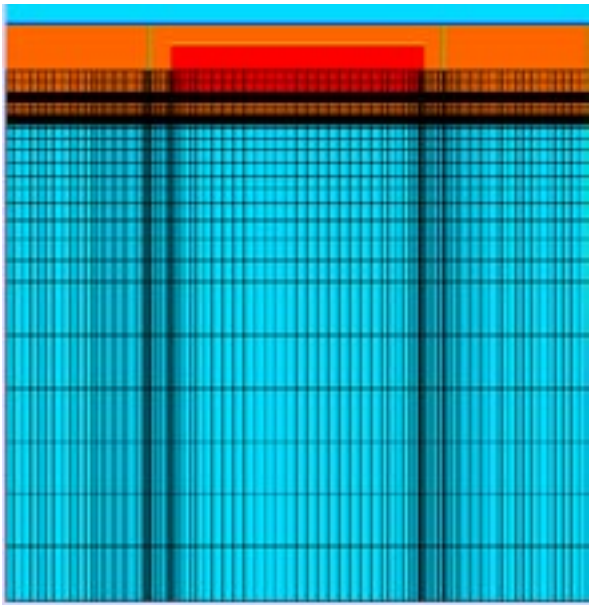

Figure 4-2. *Grid and material types (canister red, bentonite orange and rock blue). Infinite canister queue model.*

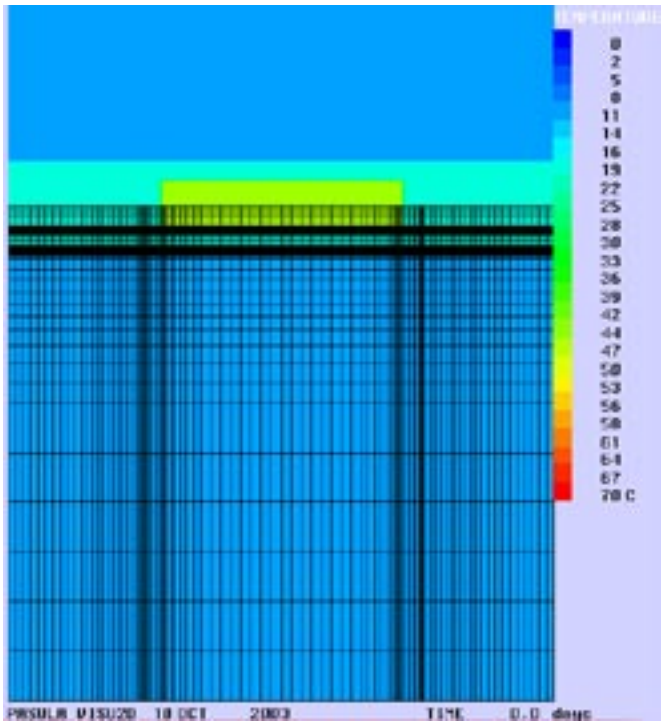

Figure 4-3. *Initial temperature distribution. Infinite canister queue model.*

Figure 4-4 shows the temperature distribution after 7 and 14 days. The outer radius 10 m of the model was great enough to avoid heat pulse reflection from the edges.

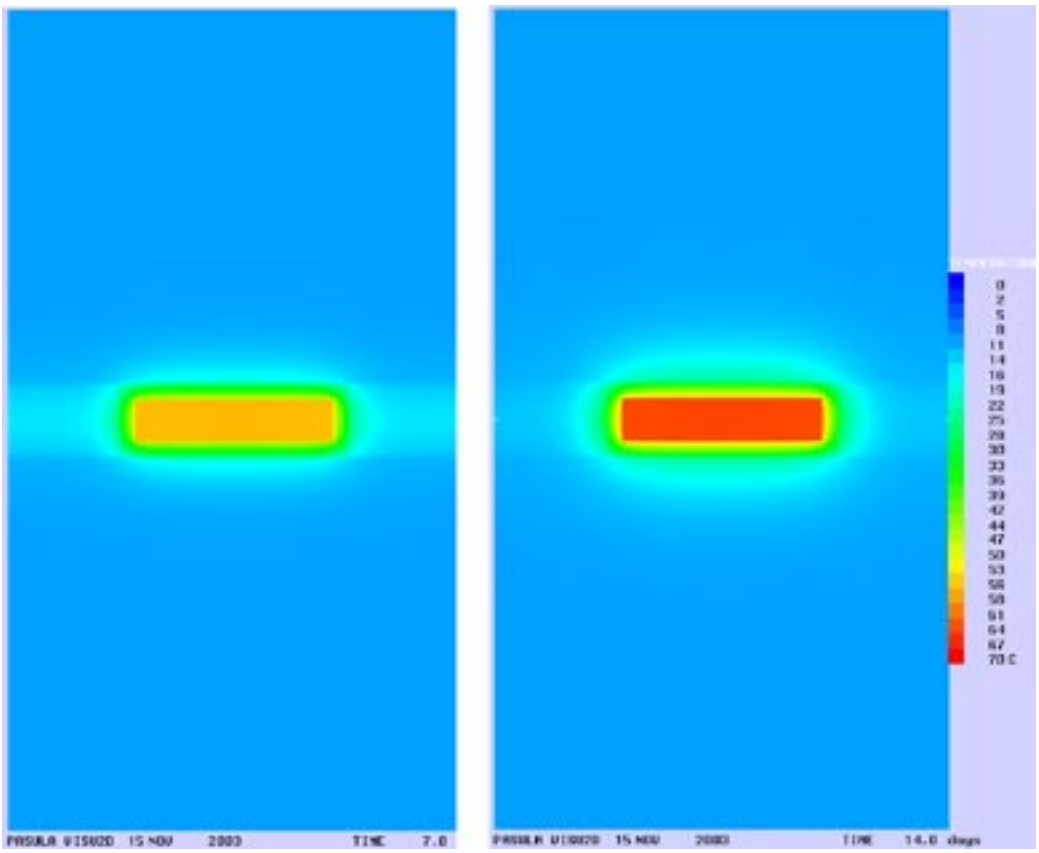

Figure 4-4. *Temperature distributions after 7 and 14 days. Infinite canister queue model.*

According to Figure 4-5 the temperature after 7 days in the middle of the canister on the outer surface of the bentonite is 30°C and on the rock surface 20°C. The temperature difference over the gap is 10°C. In the middle of the gap the temperature is about 25°C. The temperature difference over the outer gap decreases from the middle to the left or to the right, since the heat flux decreases. In the middle of the distance block the temperature difference over the gap is only about 2°C. The temperature of the canister surface increases from the initial value of 46°C to 58°C during 7 days.

Figure 4-6 shows the evolution of temperatures in the middle of a canister. Figure 4-7 shows the evolution of temperatures in middle of a distance block, where the temperature changes are small during 7 days. Figures 4-8 and 4-9 show the curves during first 30 days.

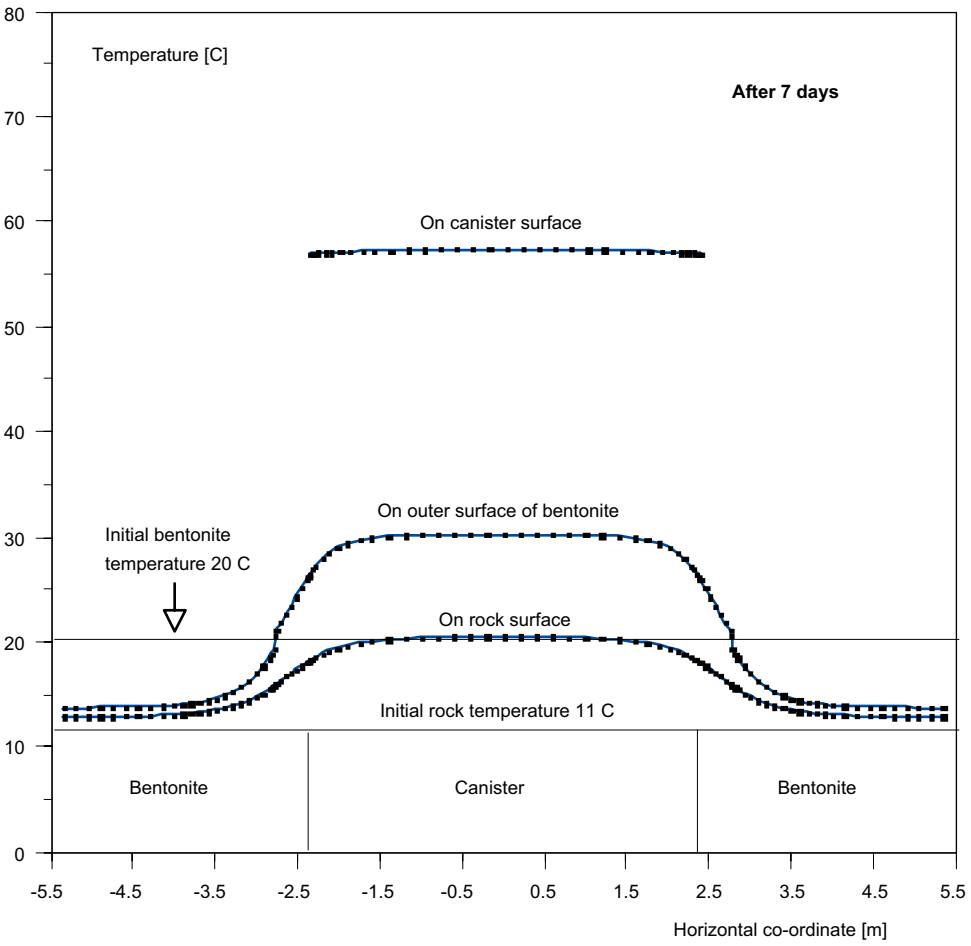

Figure 4-5. *Horizontal temperature profiles and on canister surface after 7 days (infinite queue of canisters).*

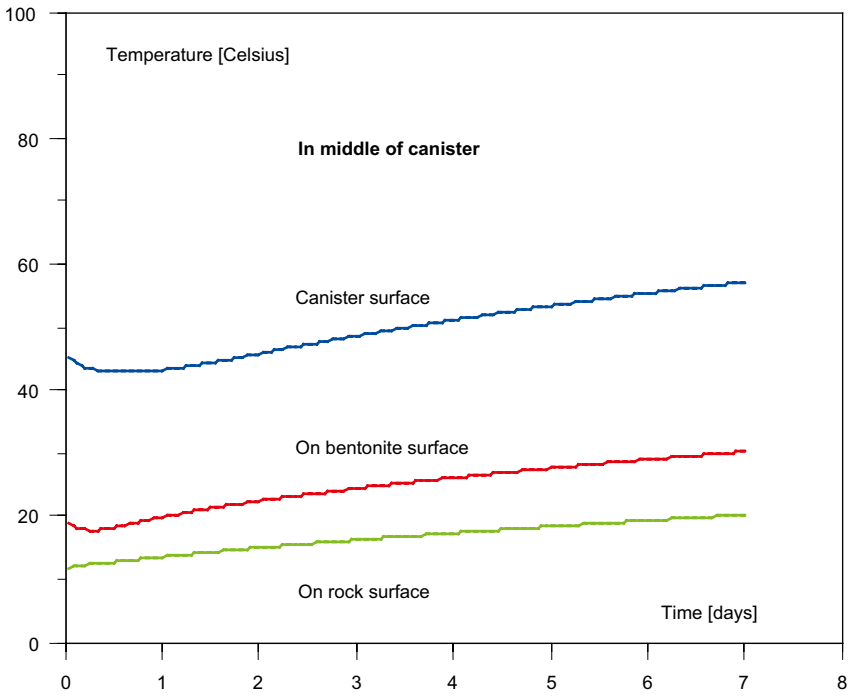

Figure 4-6. *Temperature evolution during 7 days in middle of canister (infinite queue of canisters).*

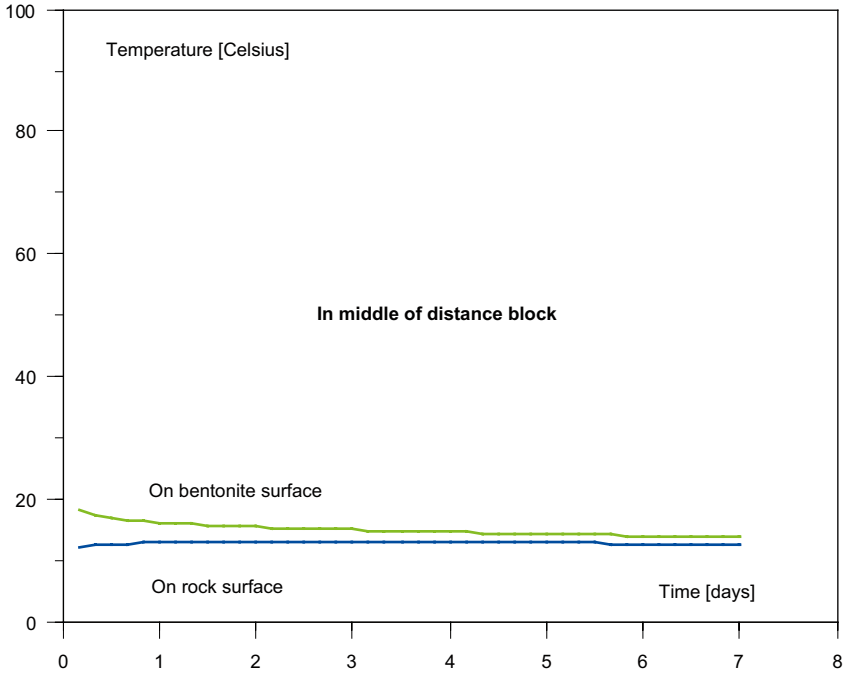

Figure 4-7. *Temperature evolution during 7 days in middle of distance block (infinite queue of canisters).*

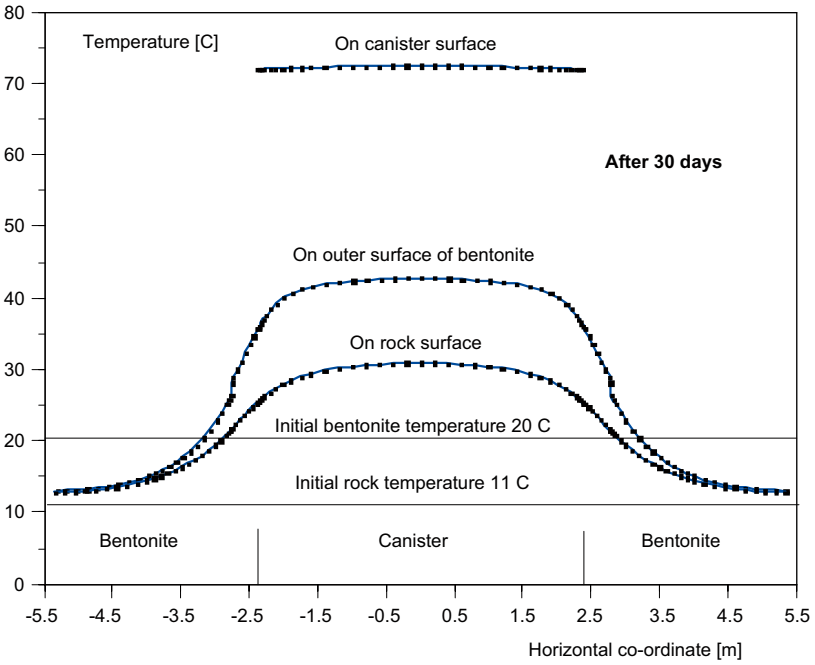

Figure 4-8. *Temperature profile in external gap and on canister surface after 30 days (infinite queue of canisters).*

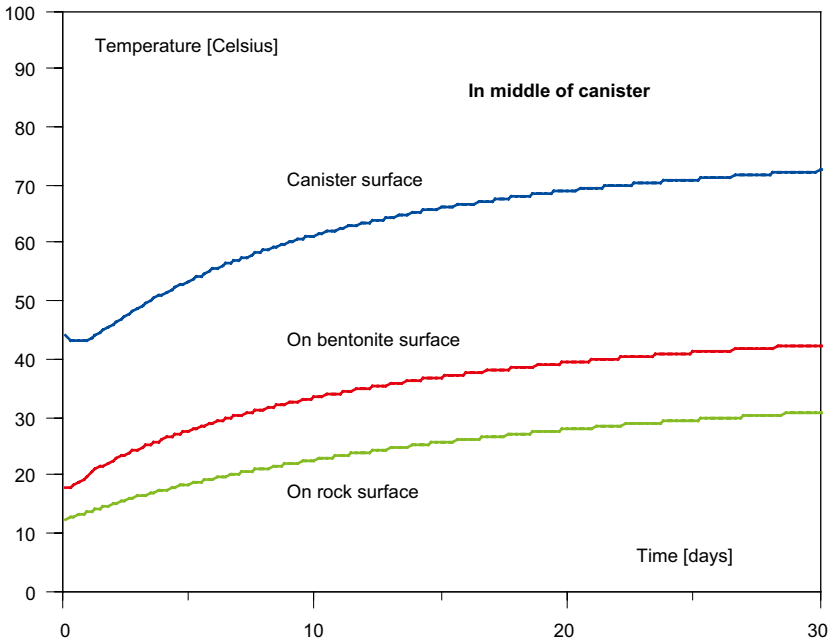

Figure 4-9. *Temperature evolution during 30 days in middle of canister (infinite queue of canisters).*

Figure 4-10 shows the temperature profile after 365 days. Temperature varies rather much in the gap against the rock. In the middle of the canister the temperature on the rock surface is 41°C and on the outer bentonite surface 55°C, whereas in the middle of the distance block the temperature is 24°C. There is a small temperature difference over the outer gap in the distance block since there is now more heat flux over the gap.

Uniform humidity conditions are difficult to achieve in the gap in longitudinal direction. Convection due to natural circulation of humid air in horizontal gaps between a container and the rock was not considered. Convection could reduce the temperature variation in the gap. On the other hand, the perforated steel plate has good conductivity and transfers quite well heat in horizontal gaps. Convection depends on the slope of the tunnel. Heat conveying capacity of air is very small. The actual slope of 1° of the tunnel is rather small. If there is no slope, horizontal circulation is small. In case of very good convection in the gap, the temperature would be constant in the horizontal gap. The average temperature of 36.8° in the middle of the gap is drawn in Figure 4-10.

Figure 4-11 shows temperature evolution during 365 days in the middle of the canister. The temperature difference between the rock and the outer surface of the bentonite is rather constant and of about 10s°C.

Figure 4-12 shows temperature distributions after 30 and 365 days. In the former case the outer radius of the model was 10 m and in the latter case grater and 20 m to avoid heat pulse reflection from the edges.

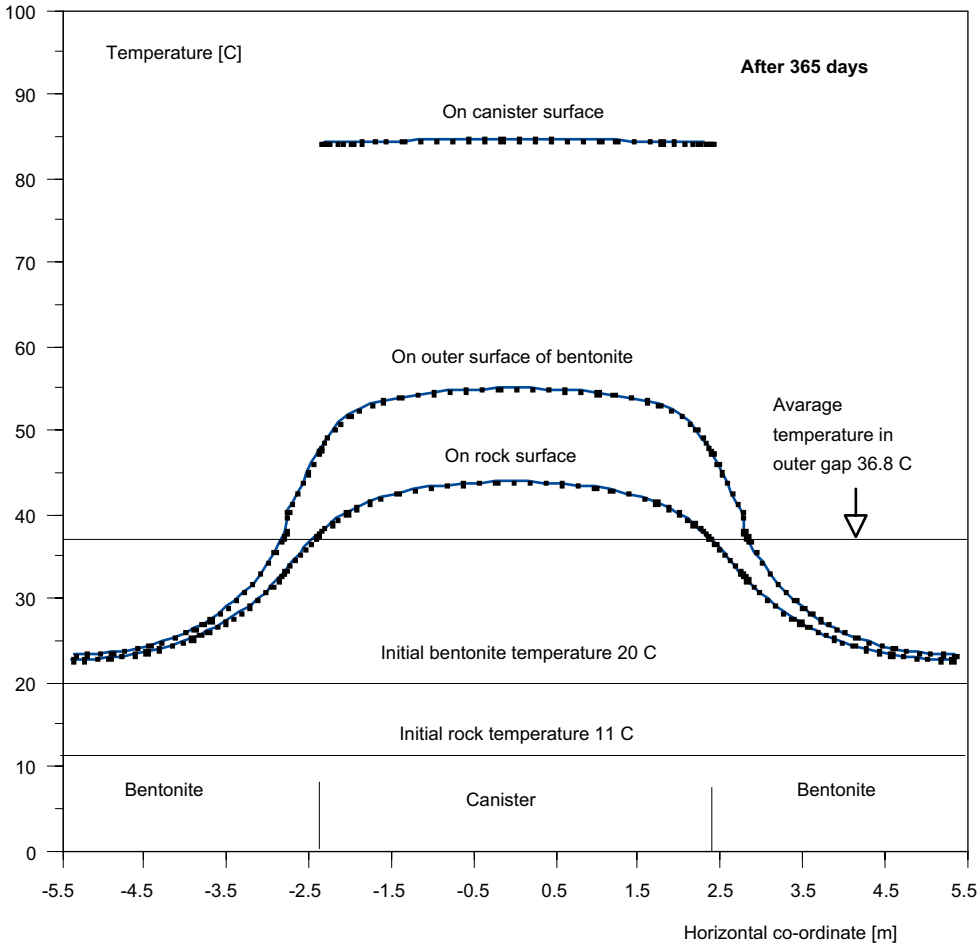

Figure 4-10. *Temperature profile in external gap and on canister surface after 365 days (infinite queue of canisters).*

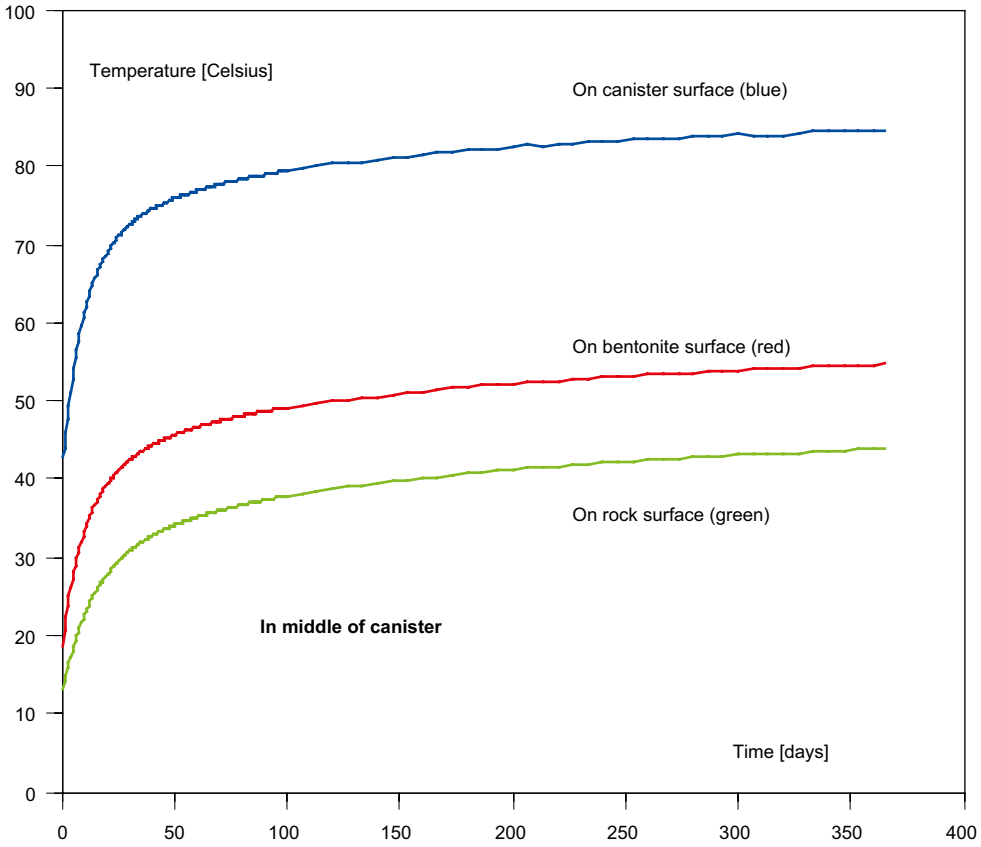

Figure 4-11. *Temperature evolution during 365 days in middle of canister (infinite queue of canisters).*

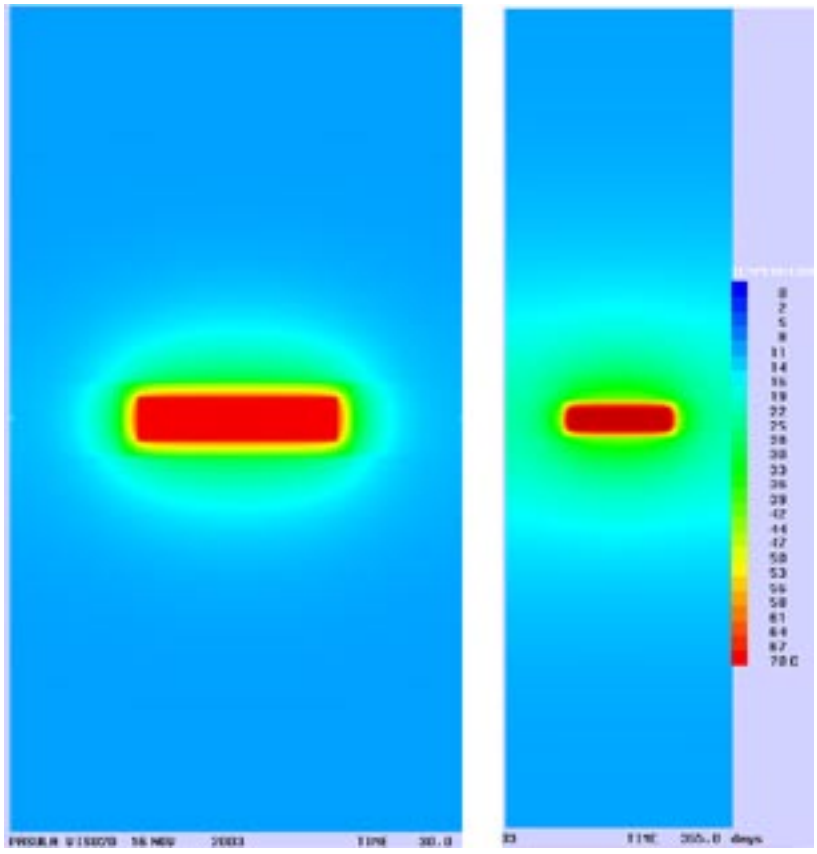

Figure 4-12. *Temperature distribution after 30 and 365 days (infinite queue of canisters).*

5 Analysis of first canister and first distance block

As mentioned earlier, the other extreme case is that the first single canister and the first distance block are only disposed. This case underestimates temperatures, since the actual number of canisters is greater than one and the canisters heat each other.

5.1 Modeling dimensions of first single canister and first distance block in open tunnel

Figure 5-1 shows the model of the first single canister and the first distance block for numerical analysis.

Figure 5-2 shows the effective conductivity λ_{eff} as a function of the temperature in the end plate against the rock. If the steel plate in the gap is omitted, the effective conductivity calculated from Equation (7) gives nearly equal conductivity (continuous line in Figure 5-2).

The effective conductivity of the 14 mm layer of the end plate against the rock and the surrounding gaps is calculated from a fitting applied (the dotted curve in Figure 5-2)

$$\lambda_{eff} = 0.073 + 6.39 \cdot 10^{-4}\, T\,. \tag{11}$$

The effective in-plane conductivity is calculated as λ_{eff} = (8 mm/14 mm)·5.2 W/m/K = 2.97 W/m/K.

The 9 mm layer of perforated steel 8 mm and the surrounding 1 mm air gap to the open tunnel (Figure 5-1) is assumed to have same thermal properties as bentonite. The error caused by this assumption is not significant, since temperatures are low on this area. Heat transfer coefficient on the surfaces in the open tunnel was assumed to be 2.0 W/m^2/°C. Heat transfer by radiation is also taken into account. The temperature in the open tunnel is assumed to be 11°C. For the emissivity of the surfaces a value of ε = 0.8 was applied leading to total emissivity of ε_{tot} = 0.667.

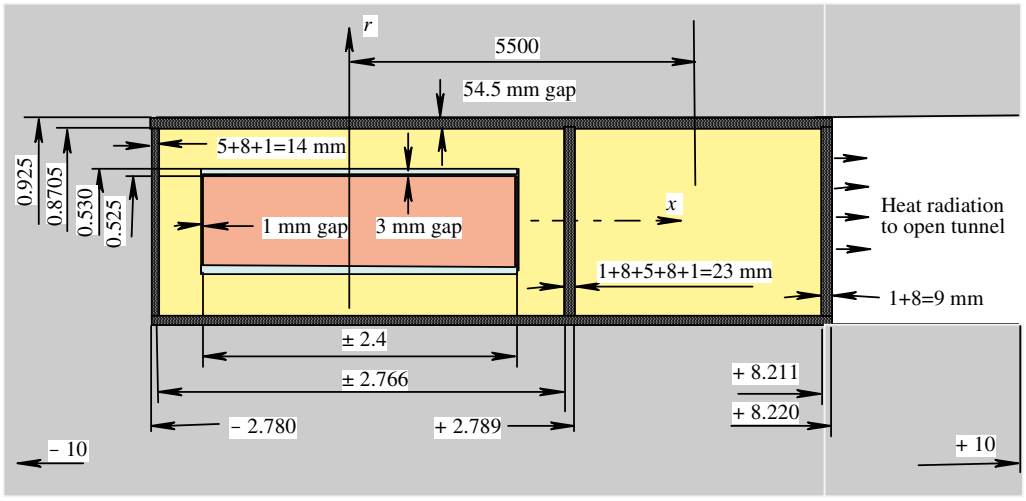

Figure 5-1. *Dimensions for the analyzing model of first single canister and first distance block.*

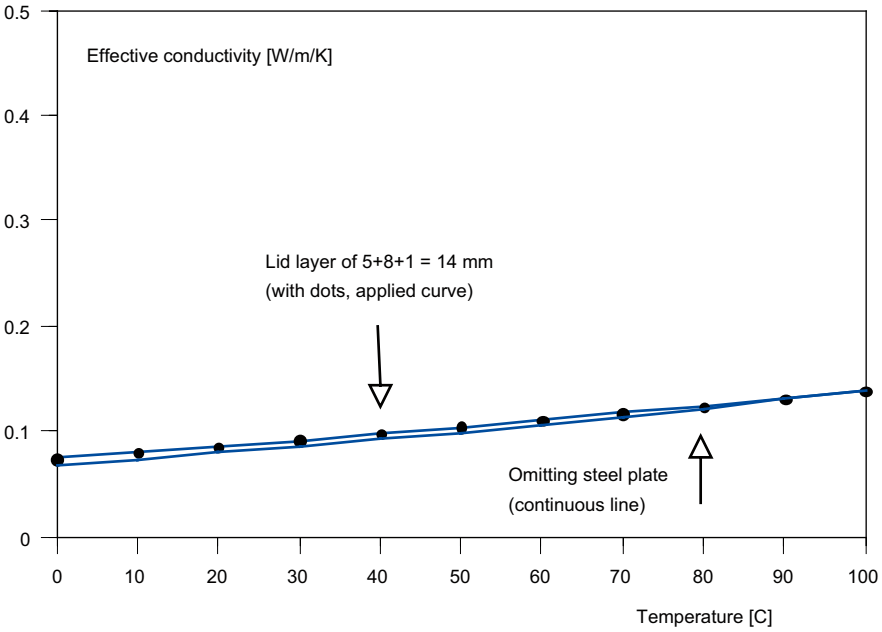

Figure 5-2. *Effective conductivity of perforated container plate and surrounding gaps.*

In the 14 mm layer against the end of the tunnel the volumetric fractions of humid air and steel are (5+0.62·8+1)/14 = 0.78 and 0.22 giving for the effective volumetric heat capacity a value of **0.67 MJ/m^3/K**, which is used in the analysis.

Figure 5-3 shows the geometry and material types of the modeled area for the numerical analysis. Figure 5-4 shows the initial temperature distribution.

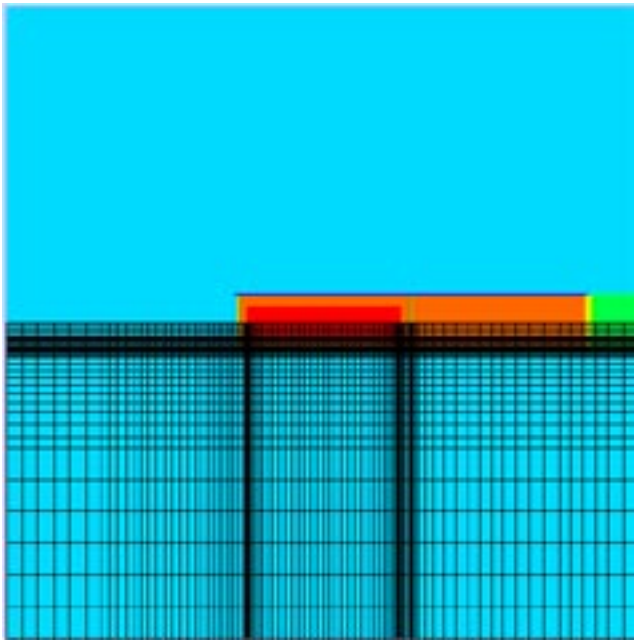

Figure 5-3. *Grid and material types (canister red, bentonite orange, rock blue and green open tunnel). First single canister and first distance block.*

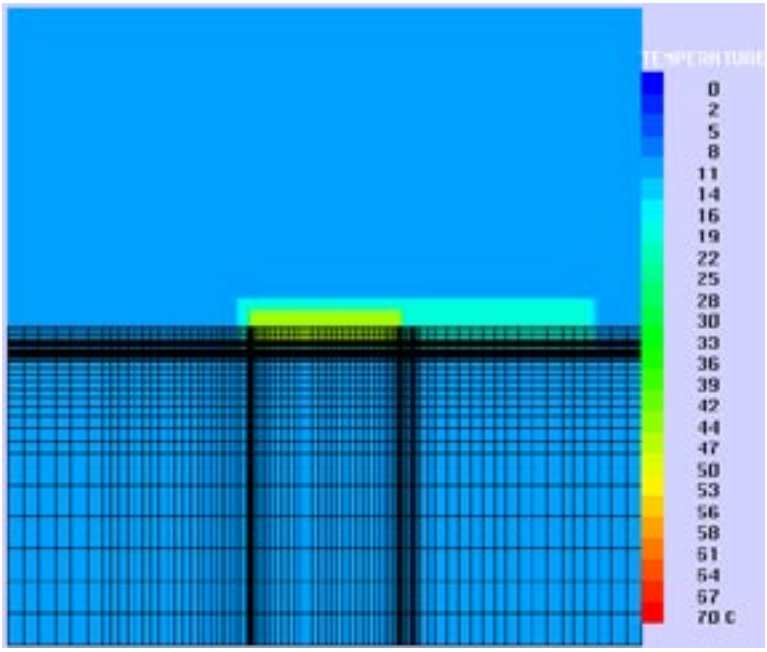

Figure 5-4. *Initial temperature distribution. First single canister and first distance block.*

Figure 5-5 shows temperature distributions after 7 and 14 days. In these cases the outer radius of the model was 10 m, whereas in case of 365 days (Figure 5-6) the outer radius was 20 m.

According to Figure 5-7 temperature distributions are rather symmetric in spite of asymmetric conditions on the left and right of the model.

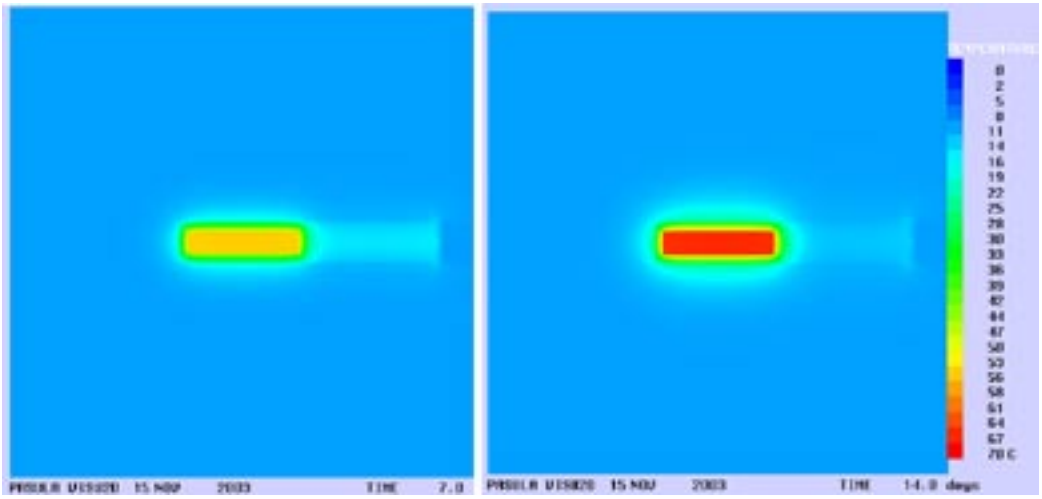

Figure 5-5. *Temperature distributions after 7 and 14 days with constant initial temperature 11°C. First single canister and first distance block.*

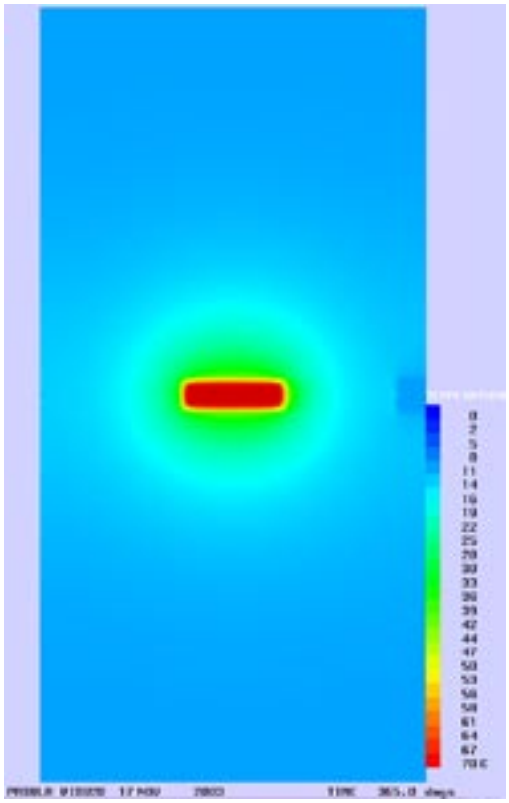

Figure 5-6. *Temperature distribution after 365 days. First single canister and first distance block.*

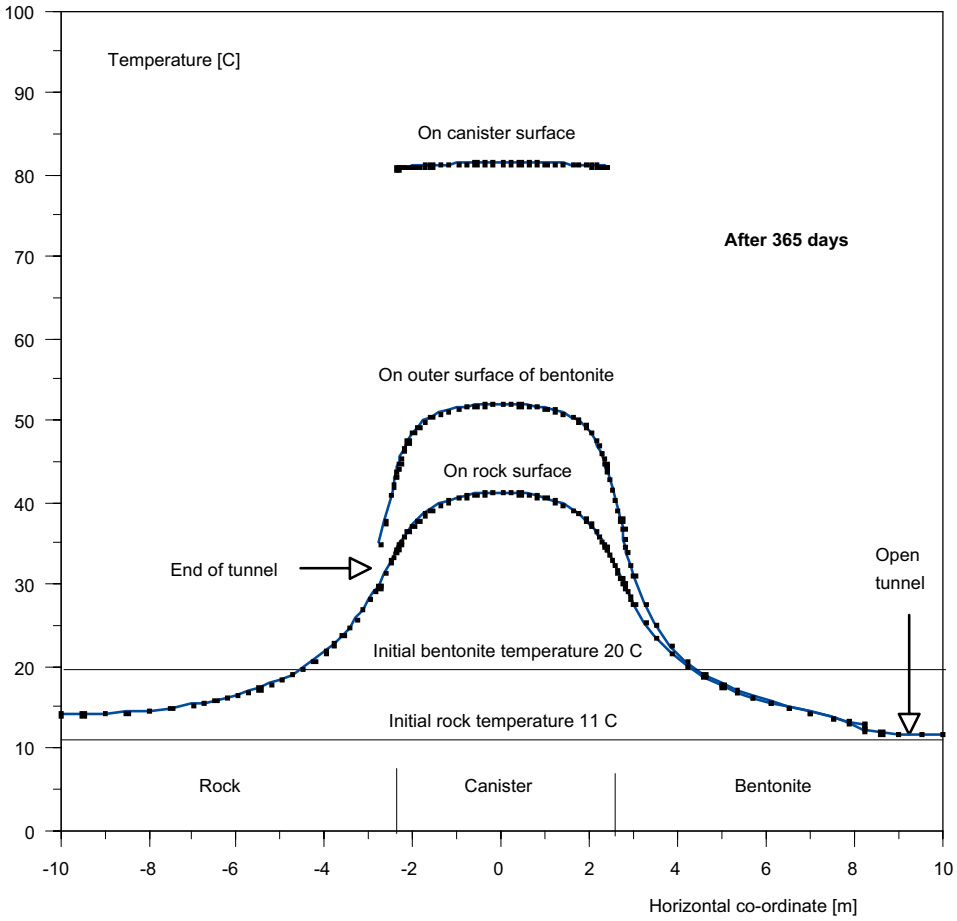

Figure 5-7. *Temperature profile in external gap and on canister surface after 365 days (first single canister and first distance block).*

5.2 Comparison between infinite canister queue and first single canister and first distance block

In the following two extreme cases are compared, where in the first case all the canisters are disposed simultaneously in an infinite queue and in the second case only the first single canister is disposed in the end of the tunnel. Figure 5-8 shows that in the external gap area the curves start to deviate from each other after tens of days in these extreme cases. Also later the differences are rather small. The actual situation in an individual canister, being much more complicated, is between these extreme cases and closer to the first case. It is not necessary to perform complicated analyses of several canisters, since the extreme cases are so close to each other's.

Figure 5-8 demonstrates that in practice the interaction of the canisters can be neglected for several months after disposal.

Figure 5-9 shows the evolution of temperatures in the middle of the distance block. Here the temperature differences between two extreme cases are much more greater than in the middle of a canister (Figure 5-8).

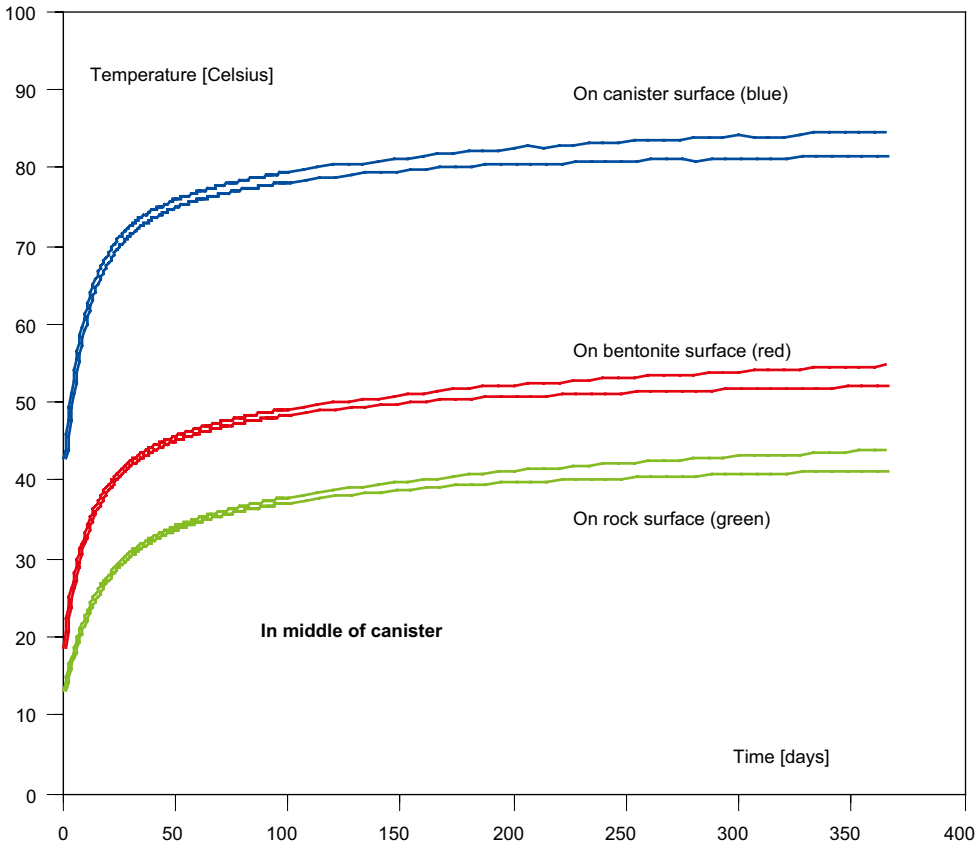

Figure 5-8. *Temperature evolution during 365 days in middle of canister. Upper curves are related to infinite canister queue and lower curves to single canister.*

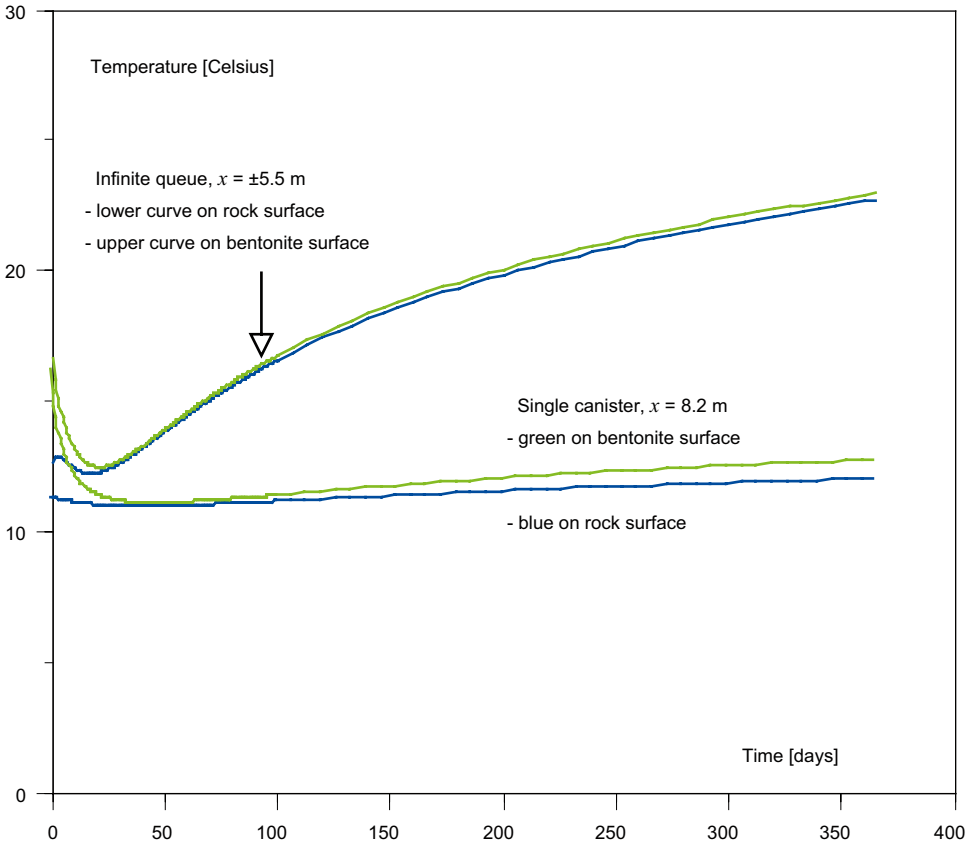

Figure 5-9. *Temperature evolution during 365 days in middle of distance block.*

6 Concluding remarks

The objective of the study was to simulate the operation phase atmospheric conditions in open horizontal tunnels, where the KBS-3H type canister containers and distance blocks are disposed. The analyses concerned BWR type canisters.

The analyses were made as heat conduction problem by taking into account radiation over gaps. A perforated steel plate surrounds a canister and bentonite. Heat transfer through a perforated plate and surrounding air gaps is a complicated three-dimensional heat transfer problem. To simplify the analysis, the gaps around a container and a distance block were taken into account by describing them by a homogenous layer having effective thermal properties.

Convection due to natural circulation of humid air in horizontal gaps between the container and rock was not considered. Convection could reduce the temperature variation in the gap. On the other hand, the perforated steel plate has good conductivity and transfers quite well heat in horizontal gaps.

Since the actual temperatures of disposal canisters depend in a complicated way on considered time and position, two extreme cases were studied to make the analyses easier. In the first extreme case an infinite queue of canisters are disposed simultaneously. This case overestimates temperatures, since the number of canisters is finite and they are not disposed simultaneously. In other extreme case only the single first canister and the first distance block are disposed. This case underestimates temperatures, since the actual number of canisters is greater than one and the canisters heat each other in later phase. The analysis showed that temperatures differ only a little from each other in the two extreme cases. Thus a complicated analysis of several canisters could be avoided. The actual situation is between the extreme cases and closer to the first case.

According to analysis the air temperature in the tunnel between the container and rock rises to range of 40–50°C within 2–3 weeks after the start of disposal operation. Temperature varies rather much axially in the gap between a container and the rock. In the middle of the canister the average temperature in the gap is about 50°C, whereas in the middle of the distance block the temperature is 24°C. Thus constant humidity conditions are difficult to achieve in the gap between a container and the rock.

Acknowledgement

Mr. Heikki Raiko from VTT Processes is gratefully acknowledged for planning the contents of the work, useful discussions and reviewing the report. Mr. Tapani Kukkola from Fortum Nuclear Services (FNS) is gratefully acknowledged for initial data and useful discussion. Mr. Jaakko Miettinen from VTT Processes is gratefully acknowledged for providing thermal properties of humid air.

References

Agelskog L, Jansson P, 1999. Heat propagation in and around the deep repository. Thermal calculation applied to three hypothetical sites: Aberg, Beberg and Ceberg. VBB Anläggning AB. SKB TR-99-02, Svensk Kärnbränslehantering AB. 35 p + App. 4 p.

Hökmark H, Fälth B, 2003. Thermal dimensioning of the deep repository. Influence of canister spacing, canister power, rock thermal properties and nearfield design on the maximum canister surface temperature. Clay Technology AB. SKB TR-03-09, Svensk Kärnbränslehantering AB.

Ikonen K, 2003a. Thermal analysis of nuclear fuel repository. Posiva report 2003-4. 61 p.

Ikonen K, 2003b. Thermal analysis of KBS-3H type repository. Posiva report 2003-11. 43 p.

Kukkonen I, 2000. Thermal properties of the Olkiluoto mica gneiss: Results of laboratory measurements. Posiva Oy. Working Report 2000-40. 28 p.

Ryti H, 1973. Heat and mass transfer. Technical handbook. K.J. Gummerus Osakeyhtiö. Jyväskylä 1973. Vol. 1, pp. 357–424. (in Finnish).

Technical handbook, 1973. K.J. Gummerus Osakeyhtiö. Jyväskylä 1973. Vol. 4, p. 212. Vol. 8, p. 254. (in Finnish).